mineralized bone matrix on both the tHA ceramics and TCPS. Even after an abundant matrix formation, the shape of the cells could easily be recognized under observation by fluorescent microscopy (Fig. 4a and c). In contrast, the MSC cultured in the absence of Dex (Dex(−)) showed no osteoblastic cell shape but did show a fibroblastic shape (Fig. 4e–h) and no evidence of matrix formation. These findings indicate that MSC can easily differentiate into osteoblasts on the surface of tHA ceramics, resulting in the formation of bone matrix under conditions of osteogenic culture. Importantly, the cascade of the differentiation of MSC can be observed equally on both tHA ceramics and TCPS.

To confirm the osteogenic differentiation of MSC on tHA ceramics, we stained the cells with alkaline phosphatase (ALP) and calcium staining (Alizarin Red S) after 2 weeks of cultivation. ALP, which is a cell surface protein, is known as an early marker for osteoblastic differentiation; calcium is the principal inorganic component of bone matrix. Faint ALP stains on both the tHA ceramics (Fig. 5e and f) and TCPS (Fig. 5g and h) were detected in the culture without Dex, but the stains were much more extensive in the culture with Dex (Fig. 5a–d). Alizarin Red S stain is commonly used to demonstrate calcium deposits. As seen in the ALP stain, the Dex-treated cells were strongly stained with Alizarin Red S (Fig. 6a–d), while the cells not treated with Dex were hardly stained (Fig. 6e–h). This biochemical data showed that the osteogenic differentiation of MSC cultured in the presence of Dex could occur on both tHA ceramic and TCPS substrata.

4. Discussion

In the progress of tissue engineering, it is important to develop new biomaterials suitable for cell cultivation. If cultured cells, especially stem cells, are to maintain their

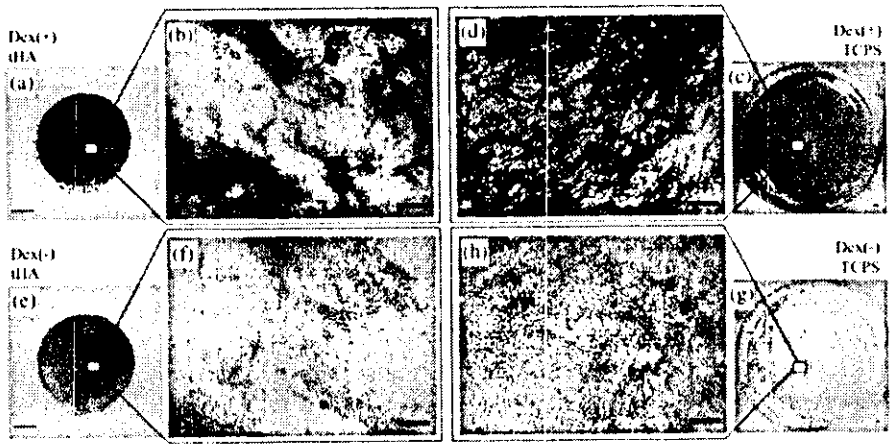

Fig. 5. Alkaline phosphatase (ALP) staining of the cultured cells on day 14. Numerous regions of the cultured cells were positive for ALP in the presence of Dex both on tHA ceramics (a, b) and TCPS (c, d). The positive areas are red. In contrast, in the absence of Dex on tHA ceramics (e, f) and TCPS (g, h), ALP activities were very low and only a few cells showed weak ALP signals. Bar: 1 mm. Double bar: 0.1 mm.

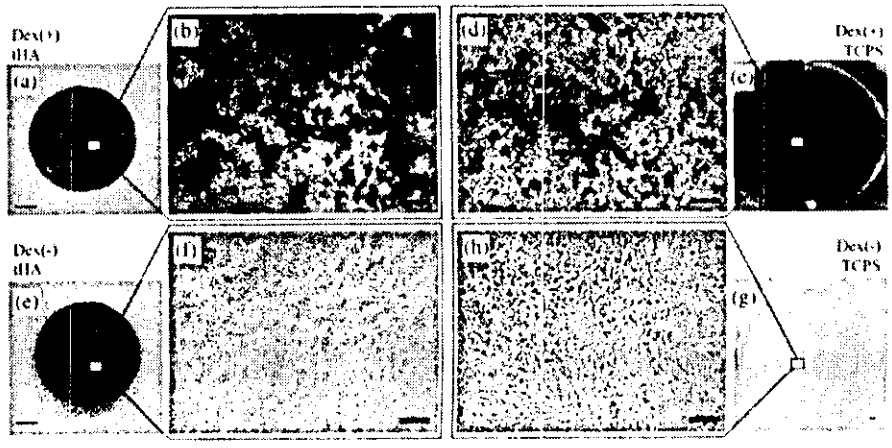

Fig. 6. Calcium staining of the cultured cells with Alizarin Red S on day 14. Many Alizarin Red stainable regions of the cultured cells could be detected in the presence of Dex on tHA ceramics (a, b) and TCPS (c, d); the stain was at almost basal levels for cells cultured in the absence of Dex on tHA ceramics (e, f) and TCPS (g, h). Bar: 1 mm. Double bar: 0.1 mm.

biological activity within the materials, they are expected to have the capability of self-renewal and differentiation into lineage-committed cells after in vivo implantation. Therefore, the combination of cultured cells and biomaterials is a key issue for successful fabrication of regenerative cultured tissues or organs. Furthermore, cell viability and proliferation on these materials is prerequisite for clinical applications. Recently, many materials have been developed for building tissue-engineered scaffolds. We have employed a variety of ceramics such as bioactive beta-tri-calcium phosphate ceramics [1], glass ceramics [10], and bio-inert alumina ceramics [11,12] beside as bioactive hydroxyapatite for hard tissue regeneration. These ceramics can be combined with rat or human mesenchymal stem cells (MSC) derived from bone marrow. The MSC can differentiate into osteoblasts not only under in vitro but also under in vivo conditions.

Cell dynamics are usually detected by observation using an ordinary light microscopy. Unfortunately, cells on many types of ceramics are difficult to observe because of the opaque nature of the ceramics. We previously utilized synthetic transparent alumina ceramics observing cell dynamics. Transparent alumina ceramics also exist naturally, known as sapphire, which consist of single-crystal Al_2O_3. But most other ceramics such as hydroxyapatite are not naturally transparent and it is difficult to create single-crystal or transparent ceramics. Although alumina ceramics are bioinert and do not exhibit bone-bonding properties, hydroxyapatite ceramics are widely known as bioactive ceramics having bone-bonding properties and are thus suitable scaffolds for culturing MSC. However, due to the opaque nature of the ceramics, cell behavior on the ceramics is difficult to observe. To overcome this drawback, the spark plasma sintering (SPS) process has recently been used for making some types of transparent ceramics, previously thought to be impossible.

Using the SPS process, we have already succeeded in fabricating tHA ceramics [7,13] and have used these ceramics for observing the cultured cells [14]. However, the results were preliminary and the cells used did not show fluorescent emission. The present results enabled us to demonstrate the cascade of cell differentiation (osteogenic differentiation) using fluorescent cells. Importantly, we were able to use a microscope to monitor the cascade of the same samples throughout the culture period. In other words, we were able to conduct real-time monitoring of cells cultured on ceramics.

We used fluorescent cells for cultivation on the tHA ceramics, which can be clearly observed with fluorescent microscopy. It is easy to observe the morphology of non-fluorescent cells on tHA ceramics by phase-contrast microscopy during initial culture periods but it is hard to make the same observations during later culture periods, especially when the culture is conducted under osteogenic conditions. The reason for this is that the cultured cells sometimes differentiate into osteoblasts, which make a calcified matrix, and the matrix masks observation of the shape of the cells on both tHA ceramics and TCPS, using a phase-contrast microscope. Consequently, we utilized EGFP-expressed rat mesenchymal stem cells whose cellular morphology can be more clearly detected, as shown in Figs. 1 and 2. These novel approaches using transparent ceramics combined with fluorescent cells emphasized the importance of observing cellular behavior on biomaterials that are to be used as tissue-engineering materials. In fact, the tHA ceramics demonstrated the immediate capability of allowing MSC to attach to the surface. The attachment led to excellent cellular proliferation that resulted in osteogenic differentiation.

Both the TCPS and tHA ceramics discussed in this paper exhibited excellent cellular attachment followed by proliferation. Many factors might be involved in the mechanisms that occur. In this regard, fibronectin is an interesting factor and is known to be essential for promoting cellular attachment and spreading on the substrate [15]. Fibronectin is any of a group of widely distributed glycoproteins that serve as a substrate to promote cellular adhesion and migration through its central-binding domain RGD sequence [16,17]. It can be produced by most mesenchymal and epithelial cells and is also present in serum used in the culture. The interaction of fibronectin with unmodified polystyrene (as is commonly used for bacterial agar plates) is weak and about $\frac{1}{10}$ as effective in cell binding in comparison with polystyrene modified for tissue culture plates (TCPS). This is the reason that cells generally fail to grow on bacterial grade plates. Therefore, TCPS is an excellent substratum for cell culture and was therefore used as a positive control in this study. Cell attachment to tHA ceramic surfaces and the cell shape on the ceramics were quite similar to that on TCPS. This observation, as mentioned above, was easily detected by fluorescence microscopy without the need for a fixation step at any time during the culture period. This suggests that tHA ceramic surfaces are equivalent to culture-grade dishes and have the capability of supporting cellular adhesion and proliferation, which results in the osteogenic differentiation of the MSC. Although further experiments are required to clarify the mechanisms of the excellent properties of tHA, cell-binding factors such as fibronectin and laminin might easily be adsorbed on the surface of tHA ceramics, and promote the adhesion and/or proliferation of the cells on the surface.

The composite of biomaterials and cells can be applied for the treatments in a variety of clinical situations. In particular, we have succeeded in differentiating patients' derived mesenchymal stem cells (MSC) into osteoblasts together with forming bone matrix on various ceramics. Importantly, the constructs

having the cells/matrix (*regenerative cultured bone*) can be made from not only fresh cells but also cryopreserved cells from a geriatric patient's marrow cells [6]. Evidence of adequate cellular functions before their implantation into a patient is strongly needed in order to go through cell-based therapy and tissue engineering. Here, we demonstrated for the first time that transparent hydroxyapatite ceramics enable us to observe living cells directly and the ceramic surface clearly support the attachment/proliferation/differentiation of the MSC. Therefore, these results confirm the excellent properties of the hydroxyapatite ceramics to be used in hard tissue regeneration.

5. Conclusion

We used transparent hydroxyapatite (tHA) ceramics as a cell culture substrate. The ceramics make us possible to observe cell behavior on ceramics by light microscopy with ease. In this report, rat mesenchymal stem cells (rMSC) were applied and as a result, cell attachment, proliferation, and osteogenic differentiation of rMSC on tHA observed by light microscopy were significantly similar to those on tissue culture polystyrene (TCPS) dish, which is the gold standard material for cell culture. The observation of living cells on tHA is a new significant and revealed reliable nature of the hydroxyapatite ceramics for the purpose of tissue engineering in hard tissue repair.

Acknowledgements

We thank our colleagues at the National Institute of Advanced Industrial Science and Technology (AIST) and at Graduate School of Medicine; Yamaguchi University. This work was supported by the Three-Dimensional Tissue Module Project of METI (a Millennium Project) and Grant-in-Aid for Scientific Research Japan.

References

[1] Ohgushi H, Okumura M, Tamai S, Shors EC, Caplan AI. Marrow cell induced osteogenesis in porous hydroxyapatite and tricalcium phosphate. J Biomed Mater Res 1990;24:1563–70.

[2] Ohgushi H, Okumura M, Yoshikawa T, Inoue K, Senpuke N, Tamai S. Bone formation process in porous calcium carbonate and hydroxyapatite. J Biomed Mater Res 1992;26:885–95.

[3] Ohgushi H, Caplan AI. Stem cell technology and bioceramics: from cell to gene engineering. J Biomed Mater Res 1999;48:913–27.

[4] Mendes SC, Tibbe JM, Veenhof M, Bakker K, Both S, Platenburg PP, Oner FC, De Bruijn JD, Van Blitterswijk CA. Bone tissue-engineered implants using human bone marrow stromal cells: effect of culture conditions and donor age. Tissue Eng 2002;8:911–20.

[5] de Bruijn JD, van den Brink I, Mendes S, Dekker R, Bovell YP, van Blitterswijk CA. Bone induction by implants coated with cultured osteogenic bone marrow cells. Adv Dent Res 1999;13:74–81.

[6] Kotobuki N, Hirose M, Takakura Y, Ohgushi H. Cultured autologous human cells for hard tissue regeneration: preparation and characterization of mesenchymal stem cells from bone marrow. Artif Organs 2004;28:33–9.

[7] Ioku K, Kawagoe D, Toya H, Fujimori H, Goto S, Ishida K, Mikuni A, Mae H. OH-designed transparent apatite ceramics prepared by spark plasma sintering. Trans Mater Res Soc Jpn 2002;27:447–9.

[8] Maniatopoulos C, Sodek J, Melcher AH. Bone formation in vitro by stromal cells obtained from bone marrow of young adult rat. Cell Tissue Res 1988;254:317–30.

[9] Ohgushi H, Dohi Y, Kaduda T, Tamai S, Tabata S, Suwa Y. In vitro bone formation by rat marrow cell culture. J Biomed Mater Res 1996;32:333–40.

[10] Ohgushi H, Dohi Y, Yoshikawa T, Tamai S, Tabata S, Okunaga K, Shibuya T. Osteogenic differentiation of cultured marrow stromal stem cells on the surface of bioactive glass ceramics. J Biomed Mater Res 1996;32:341–8.

[11] Ohgushi H, Yoshikawa T, Nakajima H, Tamai S, Dohi Y, Okunaga K. Al_2O_3 doped apatite-wollastonite containing glass ceramic provokes osteogenic differentiation of marrow stromal stem cells. J Biomed Mater Res 1999;44:381–8.

[12] Kitamura S, Ohgushi H, Hirose M, Funaoka H, Takakura Y, Ito H. Osteogenic differentiation of human bone marrow-derived mesenchymal cells cultured on alumina ceramics. Artif Organs 2004;28:72–82.

[13] Ioku K, Yoshimura M, Somiya S. Microstructure and mechanical properties of hydroxyapatite ceramics with zirconia dispersion prepared by post-sintering. Biomaterials 1990;11:57–61.

[14] Kotobuki N, Kawagoe D, Fujimori H, Goto S, Ioku K, Ohgushi H. In vitro osteogenic activity of rat bone marrow derived mesenchymal stem cells cultured on transparent hydroxyapatite ceramics. Key Eng Mater 2004;254:1055–8.

[15] Moser R, Fehr J, Olgiati L, Bruijnzeel PL. Migration of primed human eosinophils across cytokine-activated endothelial cell monolayers. Blood 1992;79:2937–45.

[16] Dennis JE, Haynesworth SE, Young RG, Caplan AI. Osteogenesis in marrow-derived mesenchymal cell porous ceramic composites transplanted subcutaneously: effect of fibronectin and laminin on cell retention and rate of osteogenic expression. Cell Transpl 1992;1:23–32.

[17] Dennis JE, Caplan AI. Porous ceramic vehicles for rat-marrow-derived (*Rattus norvegicus*) osteogenic cell delivery, effects of pretreatment with fibronectin or laminin. J Oral Implant 1993;19:106–15.

Cell Transplantation, Vol. 13, pp. 367–376, 2004
Printed in the USA.

0963-6897/04 $20.00 + .00

Bone Tissue Engineering Using Novel Interconnected Porous Hydroxyapatite Ceramics Combined With Marrow Mesenchymal Cells: Quantitative and Three-Dimensional Image Analysis

Masataka Nishikawa,* Akira Myoui,* Hajime Ohgushi,† Masako Ikeuchi,†
Noriyuki Tamai,* and Hideki Yoshikawa*

*Department of Orthopaedics, Osaka University Graduate School of Medicine,
2-2 Yamadaoka, Suita City, Osaka 565-0871, Japan
†Tissue Engineering Research Center, National Institute of Advanced Industrial Science and Technology,
3-11-46 Nakouji, Amagasaki City, Hyogo 661-0974, Japan

We developed fully opened interconnected porous calcium hydroxyapatite ceramics having two different pore sizes. One has pores with an average size of 150 μm in diameter, an average 40-μm interconnecting pore diameter, and 75% porosity (HA150). The other has pores with an average size of 300 μm in diameter, an average 60–100-μm interconnecting pore diameter, and 75% porosity (HA300). Because of its smaller pore diameter, HA150 has greater mechanical strength than that of HA300. These ceramics were combined with rat marrow mesenchymal cells and cultured for 2 weeks in the presence of dexamethasone. The cultured ceramics were then implanted into subcutaneous sites in syngeneic rats and harvested 2–8 weeks after implantation. All the implants showed bone formation inside the pore areas as evidenced by decalcified histological sections and microcomputed tomography images, which enabled three-dimensional analysis of the newly formed bone and calculation of the bone volume in the implants. The bone volume increased over time. At 8 weeks after implantation, extensive bone volume was detected not only in the surface pore areas but also in the center pore areas of the implants. A high degree of alkaline phosphatase activity with a peak at 2 weeks and a high level of osteocalcin with a gradual increase over time were detected in the implants. The levels of these biochemical parameters were higher in HA150 than in HA300. The results indicate that a combination of HA150 and mesenchymal cells could be used as an excellent bone graft substitute because of its mechanical properties and capability of inducing bone formation.

Key words: Bone tissue engineering; Hydroxyapatite; Image analysis; Marrow mesenchymal cell; Osteoblast; Osteoconduction

INTRODUCTION

The ideal bone graft is autogenous bone but there are many problems, such as quantitative limitations of the graft and the inevitable invasion of normal tissues to harvest the graft bone. To avoid these problems, synthetic hydroxyapatite (HA) ceramics have been used as bone graft substitutes in orthopedic, craniofacial, and dental applications (1,3,7,10,21). HA ceramics are known to be biocompatible, osteoconductive, and bioactive, with bone bonding directly to the surface of the ceramics (4,8,22). However, only a few researchers have reported that the pores of implanted ceramics were completely filled with the newly formed host bone (22). It would be reasonable to assume that the reason for this is the nonuniform pore geometry and few interpore connections of conventional synthetic HA ceramics. The size of the interpore connections rather than the size of the pores themselves might be the primary limiting factor of osteoconduction into the central area of HA ceramic blocks. This is because interpore connections under 3 μm in diameter do not permit cell migration and vascularization into the pores, events essential for new bone formation (20).

We recently developed fully open interconnected porous calcium hydroxyapatite ceramics (IP-CHA) and reported the resulting superior osteoconduction by permitting cells and tissues to invade deep into the pores (20). However, not all of these ceramics are osteoinductive and, therefore, the applications are limited. In this re-

Address correspondence to Hajime Ohgushi, M.D., Ph.D., Tissue Engineering Research Center, National Institute of Advanced Industrial Science and Technology, 3-11-46 Nakouji, Amagasaki City, Hyogo 661-0974, Japan. Tel: (+81) 6-6494-7806; Fax: (+81) 6-6494-7861; E-mail: hajime-ohgushi@aist.go.jp

gard, we have reported on the osteogenic capability of fresh marrow cells or culture-expanded marrow mesenchymal cells, which combined with porous HA ceramics. Such composites showed ectopic bone formation in the pore areas of the HA ceramics (11,13,14,18,24,25). Importantly, the composites also demonstrated their healing potential when implanted into a site in which there is a bony defect (12). Due to the interconnected porous structure of IP-CHA, osteogenic cells can be appropriately introduced within the pores and are thus useful as a scaffold in bone tissue engineering. In this study, IP-CHA, having two different pore sizes, were combined with marrow mesenchymal cells and evaluated for their osteogenic capability.

MATERIALS AND METHODS

Materials

Fully open IP-CHA were synthesized by adopting a "foam-gel" technique from a slurry of hydroxyapatite (60 wt%) with a cross-linking substrate (polyethyleneimine, 40 wt%), as previously reported (20). The solid and porous components of the microstructure were completely interconnected. We prepared two types of IP-CHA. One had pores averaging 150 μm in diameter, an average 40-μm interconnecting pore diameter, and 75% porosity (HA150). The other had pores averaging 300 μm in diameter, 60–100-μm interconnecting pore diameter, and 75% porosity (HA300).

For comparison, we purchased three different commercially available synthetic porous hydroxyapatite ceramics (HA-A, HA-B, and HA-C), which have been used in orthopedic or dental surgery in Japan. HA-A has an average pore diameter of 300 μm and 50% porosity. HA-B has an average pore diameter of 200 μm and 70% porosity. HA-C has pore with diameters of 50–300 μm and 35–48% porosity.

Blocks of these ceramics (HA150, HA300, HA-A, HA-B, and HA-C) were cut and shaped into 5-mm-diameter disks that were 2 mm thick.

Mercury Porosimetry

The distribution of the interpore connections in hydroxyapatite ceramics was measured from the penetration of Hg liquid in an evacuated porosimeter (pore sizer, 9310, Shimadzu Co., Kyoto, Japan) as previously described by Tamai et al. (20). The available pores that were connected by interpore connection >10 μm in diameter were calculated by the following equation: available porosity (%) = total porosity (%) – unavailable porosity (%) (the inaccessible pore space calculated by integrating the cumulative volume of pores that were connected with interpore connections <10 μm in a diameter, according to the result of mercury porosimeter).

Marrow Cell Preparation and Culture

Marrow cells were obtained from the bone shaft of the femora of 7-week-old Fischer 344 male rats. Both ends of the femur were cut away from the epiphysis, and the marrow was flushed out using 10 ml of culture medium expelled from a syringe through a 21-gauge needle, according to the method developed by Maniatopoulos et al. (9). The released cells were collected in two T-75 flasks (Costar, Cambridge, MA) containing 15 ml of the standard medium described below. The medium was changed after 24 h to remove hematopoietic cells. Subsequently, the medium was renewed three times a week. Cultures were maintained in a humidified atmosphere of 95% air with 5% CO_2 at 37°C.

The standard medium consisted of Eagle's minimal essential medium (MEM) containing 15% fetal bovine serum (JRH Bioscience, Lenexa, KS, Lot No.002095) and antibiotics (100 U/ml of penicillin, 100 μg/ml of streptomycin, and 0.25 μg/ml of amphotericin B; Sigma Chemical Co., St. Louis, MO).

After 7 days in primary culture, adherent marrow mesenchymal cells (MMCs) were released from the culture substratum using 0.1% trypsin. The cells were concentrated by centrifugation at 900 rpm for 5 min at 4°C and resuspended at 10^6 cells/ml. The 24 ceramic disks were soaked in 4 ml of cell suspension (10^6 cells/ml) overnight in a CO_2 incubator.

After the overnight incubation, the disks were transferred into a 24-well plate (Falcon, Franklin Lakes, NJ) for subcultures. Each ceramic was subcultured in one well with 1 ml of the standard medium supplemented with 10 mM of β-glycerophosphate, disodium salt, pentahydrate (Calbiochem, Darmstadt, Germany), 82 μg/ml of L-ascorbic acid phosphate magnesium salt *n*-hydrate (Wako Pure Chemical Industrials, Osaka, Japan), and 10^{-8} M of dexamethasone (Dex, Sigma Chemical Co.). To evaluate the efficiency of the dexamethasone, the subcultures without Dex were used as in vitro controls. The medium was renewed three times a week, and the subcultures were maintained for 2 weeks. These subcultured MMCs in the ceramic disks were washed twice with phosphate-buffered saline (Gibco, Invitrogen Corporation, Grand Island, NY) and prepared for measurement of alkaline phosphatase (ALP) activity to evaluate if the HA ceramics support in vitro osteoblastic differentiation of marrow mesenchymal cells.

Implantation

Syngeneic 7-week-old male Fischer 344 rats were anesthetized by intramuscular injection of ketamine (45 mg/kg) and xylazine (9 mg/kg). Five ceramic disks cultured with MMCs in the presence of Dex for 2 weeks were implanted subcutaneously at five sites into the back of each syngeneic rat and five ceramic disks with-

out MMCs were also implanted as controls. The rats were sacrificed at 2, 4, 6, and 8 weeks after implantation, and the implants were harvested from each experimental group for biochemical and histological assay. All procedures used in the animal experiments complied with the standards given in the Osaka University Medical School Guidelines for the Care and Use of Laboratory Animals.

Histological Examination

To obtain decalcified sections, 5 implants harvested from each group at 2, 4, 6, and 8 weeks were fixed in 10% buffered formalin, decalcified with K-CX solution (Falma Co., Tokyo, Japan), and embedded in paraffin. They were cut parallel to the round face of the implants and were stained with hematoxylin and eosin for light microscopy.

Biochemical Analysis

ALP activity was measured as reported previously (24). Each ceramic disk was crushed, homogenized in 0.2% Nonidet P-40 containing 1 mM $MgCl_2$, and centrifuged at 10,000 rpm for 1 min at 4°C. Then the supernatant was assayed for ALP using *p*-nitrophenyl phosphate as a substrate. ALP activity was represented as μmol of *p*-nitrophenol released per ceramic disk for 30 min of incubation at 37°C (19).

Osteocalcin was extracted from the sediment after extraction of 20% formic acid for 2 weeks at 4°C. An aliquot (1 ml) of the formic acid extract was then applied to a column of NAP-10 (Sephadex G-25 DNA grade, Amersham Bioscience, Uppsala, Sweden) and was eluted with 1.5 ml of 10% formic acid. Protein fractions were collected, lyophilized, and prepared for the assay of intact rat osteocalcin as previously described (6). The assay method (Rat Osteocalcin EIA Kit; No. BT-490 Biomedical Technologies Inc., Stoughton, MA) utilized two antibodies that recognized the N-and C-terminal amino acid regions of rat osteocalcin. Purified rat osteocalcin was used for standard and tracer.

Microcomputed Tomography Evaluation

Bone formed in the pore areas of the ceramics was evaluated by microcomputed tomography [micro-CT: MCT-CB100MF(Z); Hitachi Medical Corporation, Tokyo, Japan]. After fixation in 10% buffered formalin, each implant was placed as a round face facing the jig surface and scanned at intervals of every 10 μm at a voltage of 50 kV, 200 μA. The analytical condition was superprecision mode and 7× magnification with an image intensifier field of 1.8 in. After the samples were scanned, they were decalcified and prepared for the histological sections. The micro-CT image at almost the same level as the histological section was compared and the intensity of the newly formed bone in the micro-CT image was determined. Then the newly formed bone areas in the micro-CT images that matched with the histology were extracted and their volumes were measured using the software package, TRI3D-BON (Ratoc System Engineering Co., Ltd., Tokyo, Japan).

Statistical Analysis

Statistical analysis was performed using unpaired *t*-test with statistical analysis software, STATVIEW version 4.5 (SAS Institute Inc., Cary, NC). The statistical significance level was set at $p = 0.05$.

RESULTS

Evaluation of Interconnected Porosity

The distribution of the interpore connections was measured using mercury porosimetry technique. In IP-CHA, most of the interpore connections ranged from 10 to 100 μm in diameter, a dimension that theoretically would be permissive to cell migration or tissue invasion from pore to pore. The interpore connections of HA150 and HA300 had a maximum peak at 40 and 80 μm, respectively. Interpore connections >10 μm accounted for as much as 90% of the total porosities in IP-CHA. The available porosities of HA150 and HA300 were as high as 67% and 70%, respectively. However, in HA-A, HA-B, and HA-C, the maximum peaks of the interpore connections were at 22, 15, and <1 μm, respectively. In addition, the total number of the interpore connections was much less than IP-CHA. The available porosities of HA-A, HA-B, and HA-C were as low as 28.5%, 36.7%, and 2.5%.

In Vitro Osteoblastic Differentiation of MMCs

It is well known that MMCs can differentiate into osteoblasts in culture conditions with Dex (9,15). We also reported that in vitro osteoblastic differentiation can occur on the surface of many kinds of ceramics (16,17). As a result of these findings, we first examined whether the fully open interconnected porous calcium hydroxyapatite ceramics (IP-CHA) can support in vitro differentiation by measuring ALP, one of the osteoblastic markers. IP-CHA (HA150 and HA300), having two different pore sizes, were combined with MMCs and then cultured for 2 weeks in the presence or absence of Dex. As shown in Figure 1, the ALP activities of HA150 with MMCs (HA150/MMCs) and that of HA300 with MMCs (HA300/MMCs) cultured with Dex were considerably higher than those cultured without Dex throughout the culture period. The fluctuation of ALP activities of HA150/MMCs and HA300/MMCs with Dex during the culture period showed a similar pattern, but the activity of HA150/MMCs was higher than that of HA300/MMCs at 4 and 14 days after culture. These findings

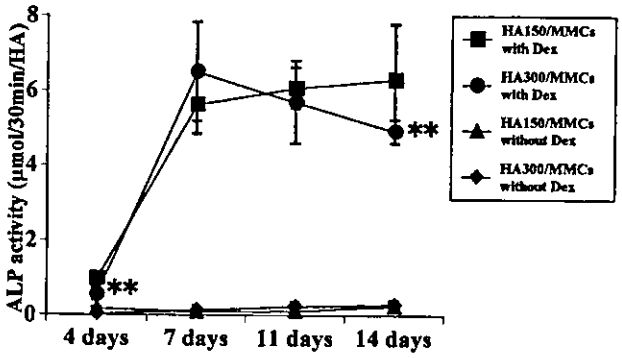

Figure 1. In vitro alkaline phosphatase activity (ALP) of fully open interconnected porous calcium hydroxyapatite (IP-CHA), which was combined with MMCs and cultured in the presence or absence of dexamethasone (Dex). Two types of IP-CHA, one with pores with an average diameter of 150 μm (HA150) and the other with pores with an average diameter of 300 μm (HA300), were used in this experiment as in vitro cell culture substrata. The culture was performed with or without Dex. ALP activity of four groups: HA150/MMCs with Dex, HA300/MMCs with Dex, HA150/MMCs without Dex, and HA300/MMCs without Dex. Data are presented as mean ± SD ($n = 5$). $^{**}p < 0.01$ vs. HA150/MMCs with Dex. All ALP activity in HA150/MMCs and HA300/MMCs without Dex was significantly lower than that of HA150/MMCs with Dex.

confirmed that both types of IP-CHA can maintain Dex-dependent in vitro osteoblastic differentiation of MMCs, and HA150 has more superior capabilities for supporting differentiation than does HA300.

Histological Analyses After In Vivo Implantation

As stated above, HA150/MMCs and HA300/MMCs can show in vitro osteoblastic differentiation under the culture condition with Dex. We also reported that the ceramic/MMCs cultured with Dex showed immediate and more copious new bone formation after in vivo implantation compared with those cultured without Dex. Therefore, we performed in vivo implantation using ceramics that were combined with MMCs and cultured for 2 weeks with Dex. After the 2-week culture, the pore surface of the ceramics could be covered with a thin layer of bone matrix together with a lining of active osteoblasts and thus we refer to these cultured ceramics as constructs (ceramics/MMCs/cult construct). As a negative control, we also implanted the ceramics without cells.

Two weeks after in vivo implantation of HA150/MMCs/cult and HA300/MMCs/cult, we were able to detect obvious bone formation in many pore areas of the ceramic (Fig. 2). Bone tissue, together with many cuboidal active osteoblasts, was observed in contact with the pore surface. Newly formed vascular vessels were also observed in some pores. This finding suggests that a capillary network had been established in the IP-CHA because of the sufficient interpore connections of the ceramics. At 8 weeks after implantation (Fig. 3A, B), the bone areas and number of osteocytes in the bone matrix increased and almost all pore areas showed bone formation. In addition, regenerated bone marrow was observed together with fat cells in many pores (Fig. 3A, B). These findings indicate the importance of porous architecture (excellent interpore connections) of IP-CHA for new bone formation. To confirm the importance of the interpore connections, we also utilized three commercially available Japanese synthetic porous hydroxyapatite ceramics (HA-A, HA-B, and HA-C). The porous architectures of these ceramics are different from IP-CHA: each pore of the commercial ceramics is not fully interconnected and have many isolated porous areas or dead-end pores. These three ceramics (HA-A, HA-B, and HA-C) were combined with MMCs and cultured with Dex for 2 weeks to make constructs of HA-A/MMCs/cult, HA-B/MMCs/cult, and HA-C/MMCs/cult. These constructs were implanted at subcutaneous sites for 8 weeks and harvested. The culture/implantation methods were the same as those applied for the constructs of HA150/MMCs/cult and HA300/MMCs/cult. In contrast to IP-CHA (Fig. 3A, B), only a few pore areas in these constructs showed newly formed bone (Fig. 3C–E). Furthermore, some pore areas did not show any newly formed tissue and were empty. Therefore, ceramics having full interpore connections (HA150 and HA300) cultured with MMCs have superior in vivo bone-forming capabilities in comparison with other ceramics (HA-A, HA-B, and HA-C) with MMCs.

Although the constructs of HA150/MMCs/cult and HA300/MMCs/cult had excellent osteogenic properties, the ceramics not combined with the cells formed only fibrovascular tissue and there was no evidence of bone formation in the pore areas of the ceramics (Fig. 4).

Biochemical Analyses After In Vivo Implantation

Histological analyses showed the in vivo osteogenic capacity of the constructs of HA150/MMCs/cult and HA-300/MMCs/cult and nonosteogenic capacity of the IP-CHA (HA150 and HA300) without MMCs. To demonstrate the quantitative analyses of the osteogenic capacity, we measured ALP activity as well as the osteocalcin contents of the implants, because ALP is known to localize on the cellular membrane of active osteoblasts and osteocalcin is the bone-specific protein produced exclusively by osteoblasts.

High levels of ALP activities could be detected in both the constructs of HA150/MMCs/cult and HA300/MMCs/cult. Both showed a peak in activity 2 weeks after implantation followed by a decrease. However, the levels of activity in HA150/MMCs/cult at 4 and 6 weeks

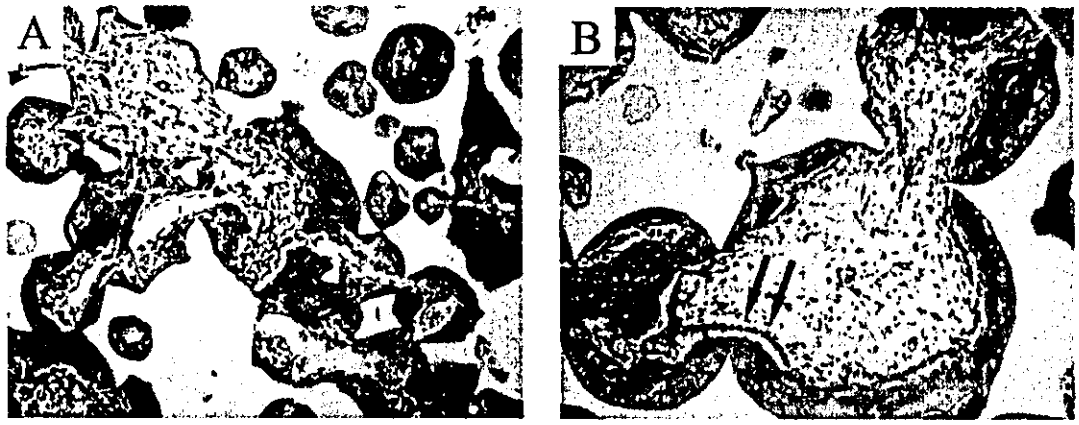

Figure 2. Histology of 2-week in vivo implanted IP-CHA construct, which was combined with MMCs and cultured with Dex. (A) The HA150/MMCs/cult construct and (B) HA300/MMCs/cult construct 2 weeks after implantation. The white area is the ghost of hydroxyapatite ceramic produced by decalcification; the black area is the bone formed in the ceramic pore areas. The arrows indicate active osteoblasts forming bone. Hematoxylin and eosin staining; original magnification ×100.

after implantation were higher than those in HA300/MMCs/cult (Fig. 5). Thus, the decrease was more evident in HA300/MMCs/cult than in HA150/MMCs/cult. The osteocalcin contents could be detected at 2 weeks after implantation of both constructs, followed by a steady increase over time. During this time, the contents of osteocalcin in HA150/MMCs/cult were always significantly higher than in HA300/MMCs/cult (Fig. 6). In

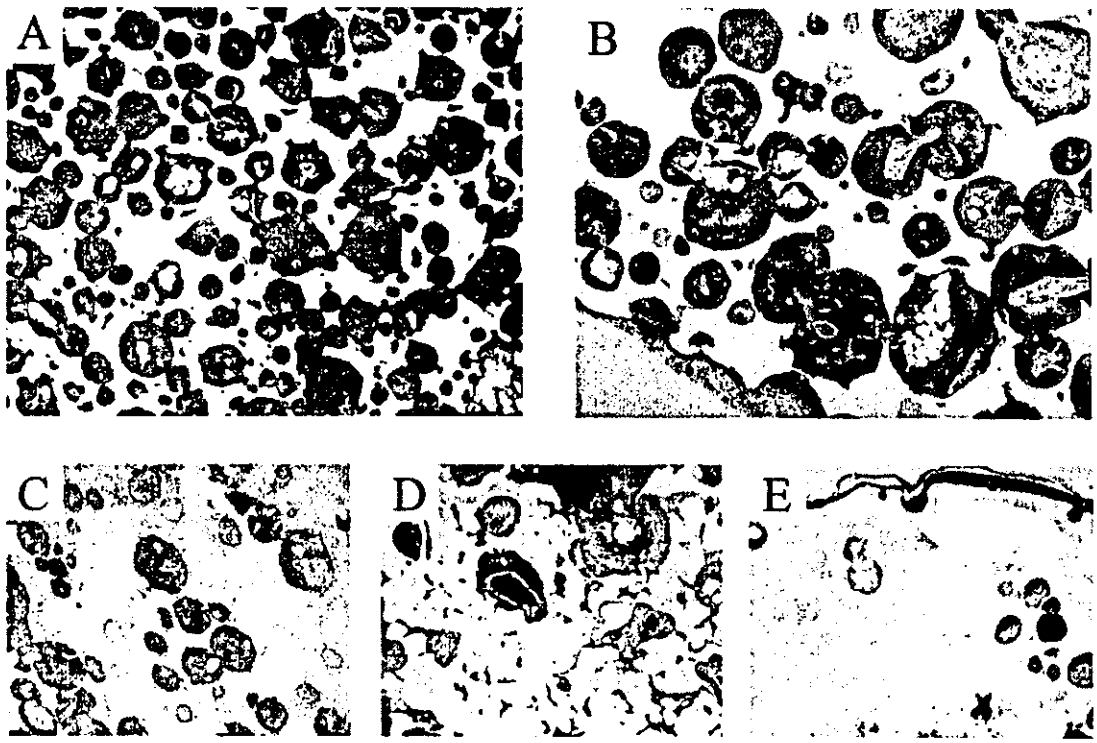

Figure 3. Histology of 8-week in vivo implant of various ceramic constructs combined with MMCs and cultured with Dex. (A) HA150/MMCs/cult, (B) HA300/MMCs/cult, (C) HA-A/MMCs/cult, (D) HA-B/MMCs/cult, (E) HA-C/MMCs/cult 8 weeks after implantation. The white area is the ghost of hydroxyapatite ceramic produced by decalcification; the black area is the bone formed in the ceramic pore areas. The HA-A/MMCs/cult, HA-B/MMCs/cult, and HA-C/MMCs/cult showed less bone formation in the pore areas compared with HA150/MMCs/cult and HA300/MMCs/cult. Hematoxylin and eosin staining; original magnification ×40.

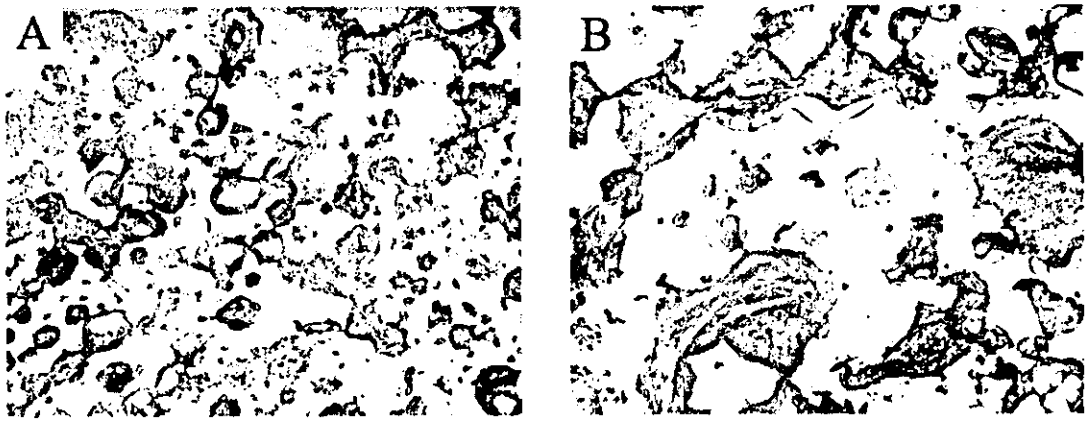

Figure 4. Histology of 8-week in vivo implanted IP-CHA without cells. (A) HA150 without cells and (B) HA300 without cells 8 weeks after implantation. In contrast to Figures 2 and 3, the IP-CHA ceramics do not show any bone formation. Hematoxylin and eosin staining; original magnification ×40.

contrast, the ALP activity and osteocalcin contents in the HA150 and HA300 without marrow cells were at basal levels. All of these results confirmed the osteogenic capacity of the constructs of IP-CHA cultured with MMCs. We used two different IP-CHA having two different pore sizes (i.e., HA150 and HA300 had mean pore diameters of 150 and 300 μm, respectively). The ALP and osteocalcin contents of HA150 combined with MMCs were more than those of HA300, meaning that HA150 had superior in vivo osteogenic capacity to that of HA300.

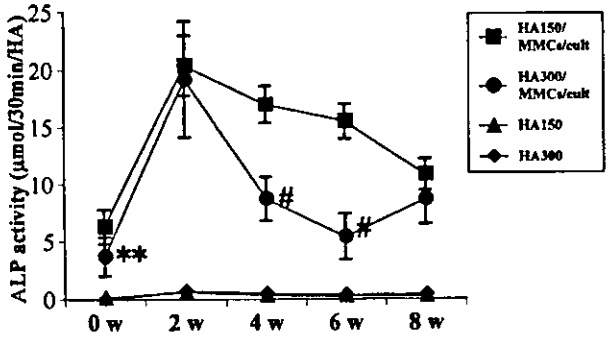

Figure 5. In vivo alkaline phosphatase (ALP) activities of implanted HA150/MMCs/cult, HA300/MMCs/cult, HA150, and HA300. IP-CHA was combined with MMCs and cultured with Dex for 2 weeks (HA150/MMCs/cult and HA300/MMCs/cult), then implanted and harvested 0–8 weeks after implantation. HA150 and HA300 without cells were also implanted as controls. The implants were used for ALP assay as described in Materials and Methods. Data are presented as mean ± SD ($n = 5$). $^{**}p < 0.01$, $\#p < 0.0001$ vs. HA150/MMCs/cult. All ALP activities in HA150 and HA300 were significantly lower than those of HA150/MMCs/cult.

Micro-CT Evaluation of Newly Formed Bone Volume

To measure the total bone volume in the constructs of IP-CHA (HA150/MMCs/cult and HA300/MMCs/cult) after in vivo implantation, we studied the micro-CT analysis. Figure 7A shows a histological section of the HA300/MMCs/cult construct 8 weeks after implantation; Figure 7B shows a micro-CT image at almost the same level of the histological section of the construct. The micro-CT images show areas having high (white), middle (gray), and low (black) intensities. After matching the histological section with the micro-CT image, we defined the white, gray, and black areas as IP-CHA (HA), newly formed bone (NB), and fibrovascular tissue with fat cells (F), respectively. The software, TRI3D-BON, turned the newly formed bone areas in Figure 7B,

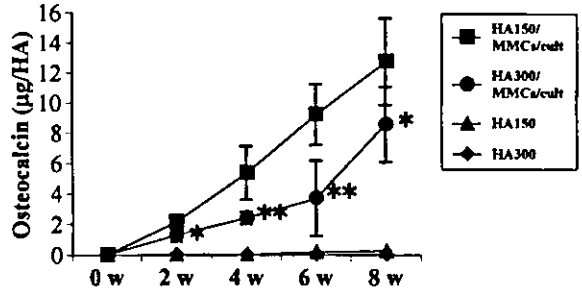

Figure 6. Osteocalcin contents of implanted HA150/MMCs/cult, HA300/MMCs/cult, HA150, and HA300. Details of the implants are described in the legend to Figure 5. The implants were used for measuring the osteocalcin contents as described in Materials and Methods. Data are presented as mean ± SD ($n = 5$). $^{*}p < 0.05$, $^{**}p < 0.01$ vs. HA150/MMCs/cult. All osteocalcin contents in HA150 and HA300 were significantly lower than those of HA150/MMCs/cult.

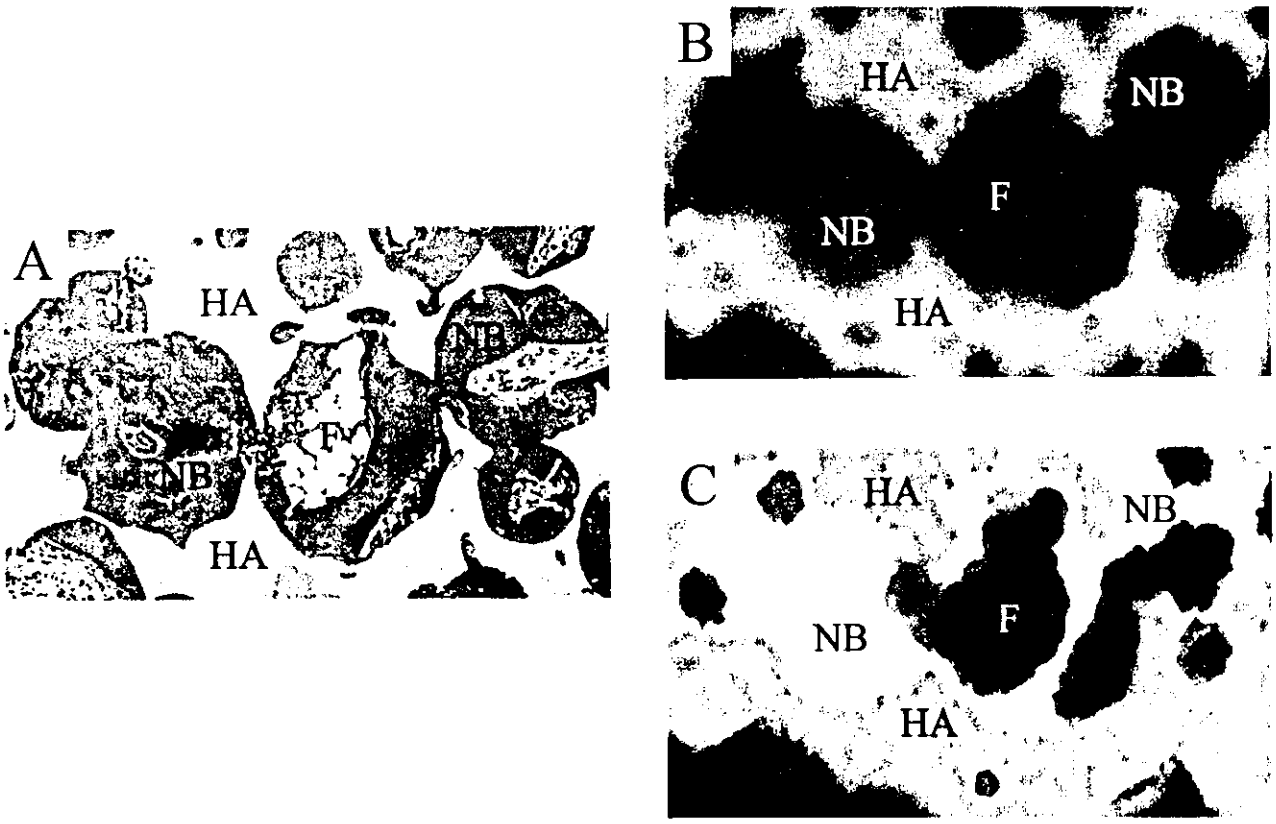

Figure 7. Micro-CT evaluation of newly formed bone in IP-CHA. (A) Histological section of HA300/MMCs/cult construct 8 weeks after implantation. Hematoxylin and eosin staining; original magnification ×100. (B) Micro-CT image at almost the same level of the histological section of the construct. (C) Same image of (B) except the gray-colored areas (newly formed bone) are represented in yellow. The micro-CT image (B) depicts the areas having a high (white), middle (gray), and low (black) intensity. By matching the image with the histological section (A), we defined the white, gray, and black areas as IP-CHA (HA), newly formed bone (NB), and soft fibrous tissue including vasculature and fat (F), respectively. Newly formed bone areas in (B) represented as gray areas were turned into yellow by the software program, TRI3D-BON, and illustrated in (C).

represented by the gray areas, into yellow, as shown in Figure 7C. We used the program to measure the yellow areas in each micro-CT section and finally calculated the total volume of yellow-colored areas, which was defined as the total volume of newly formed bone in the constructs. The yellow-colored newly formed bone in HA150/MMCs/cult and HA300/MMCs/cult could be detected 2 weeks after implantation. The bone volumes in both HA150/MMCs/cult and HA300/MMCs/cult gradually increased over time (Fig. 8). We also assembled a three-dimensional (3D) image and evaluated the distribution of newly formed bone at the sagittal section around the center of HA150/MMCs/cult and HA300/MMCs/cult 8 weeks after implantation. As shown in Figure 9, extensive newly formed bone is evident not only in the surface pore areas but also in the center pore areas in both constructs.

The newly formed bone volumes were also measured in the constructs using commercially available synthetic porous hydroxyapatite ceramics (HA-A/MMCs/cult, HA-B/MMCs/cult, and HA-C/MMCs/cult) 8 weeks after implantation. The volumes of these constructs were less than those of HA150/MMCs/cult and HA300/MMCs/cult (Table 1). These data confirmed the histological analyses shown in Figure 3.

DISCUSSION

The present results confirmed the outstanding role played by IP-CHA in supporting in vitro osteoblastic differentiation of marrow mesenchymal cells (MMCs). More importantly, the ceramics having the cultured cells (MMCs/ceramic/cult constructs) can induce new bone formation after in vivo implantation. Therefore, the constructs having osteogenic capability can be applied in massive bone defects or other cases where there is inferior repair capacity. Thus, the tissue engineering approach is very useful for the regeneration of hard tissue. This approach requires a porous scaffold to make the construct. The scaffold should be biocompatible and have sufficient initial mechanical strength to support the

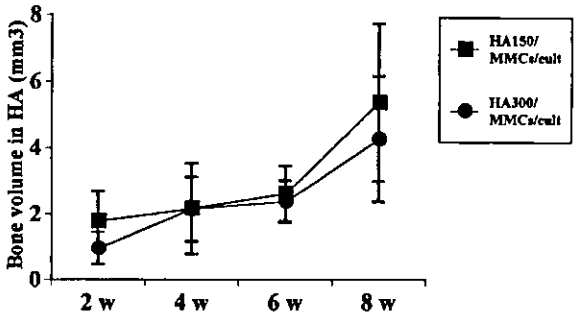

Figure 8. Bone volumes in IP-CHA determined by Micro-CT analysis. Temporal changes in bone volumes in HA150/MMCs/cult and HA300/MMCs/cult after implantation. Using the software, TRI3D-BON, we measured the yellow areas in each micro-CT section (Fig. 7C) and finally calculated the total volume of yellow, which was defined as the total volume of the newly formed bone in the constructs. The yellow-colored newly formed bone in HA150/MMCs/cult and HA300/MMCs/cult could be detected 2 weeks after implantation. The bone volumes in both HA150/MMCs/cult and HA300/MMCs/cult gradually increase with the passage of implantation time. There was no significant difference between these two constructs. Data are presented as mean ± SD ($n = 5$).

skeletal structure under weight-bearing conditions. In addition, the scaffold must have a 3D interconnected porous structure to introduce MMCs into the center of the scaffold. The MMCs should differentiate into the osteoblastic lineage.

As we have stated, an interconnected porous structure is very important in the tissue engineering approach. However, currently available commercial synthetic porous ceramics do not possess the ideal interconnected porous structure. To prove the necessity of a porous structure in supporting osteoblastic differentiation, we analyzed the in vivo bone-forming capability of porous ceramics/MMCs constructs by two different morphological approaches: the traditional histological approach and micro-CT analysis. The histological analysis is based on 2D findings of the cut section, and the extent of the bone formation areas may not accurately reflect the bone volume of the constructs because the areas depend on the cutting levels of the sample. In this regard, micro-CT can reconstruct the 3D structure of the HA ceramics, evaluate the 3D distribution of the newly formed bone, and, finally, calculate the bone volume in the ceramics. What is also important is that the analyzed samples can further be utilized for ordinal histological analysis.

As shown in the histological findings of Figures 2 and 3, the constructs of HA-A/MMCs/cult, HA-B/MMCs/cult, and HA-C/MMCs/cult showed new bone formation only in the restricted porous area near the ceramics' surface. In general, as the porosity of porous HA ceramics is higher, the interpore connection rate becomes high. However, to allow cell migration or tissue invasion from pore to pore, theoretically the diameter of the interconnection requires at least 10 μm. In this study, we measured the interpore connection of hydroxyapatite ceramics. Even highly porotic HA-B (70%) have limited interconnections of sufficient size (>10 μm) and the available porosity was as low as 36.7%. This limited interconnection may explain the poor new bone formation by the constructs using porous HA ceramics. In contrast, although the total porosity of IP-CHA was similar to HA-B, the interpore connections of IP-CHA were well controlled between 10 and 100 μm in diameter and the available porosity was from 67% to 70%. The constructs of HA150/MMCs/cult and HA300/MMCs/cult showed extensive bone formation in most pore areas regardless of location (i.e., the bone appeared in both the surface and center pore areas). This uniform appearance of the newly formed bone in most pore areas of the fully open IP-CHA is also revealed by micro-CT analysis. As shown in Figure 9, at the sagittal section of these constructs, excellent bone formation was seen at both the surface and center pore areas. Quantitative micro-CT analysis of bone formed in all constructs showed more bone formation in the HA150/MMCs/cult and HA300/MMCs/cult constructs than in other constructs (Table 1). These two different morphological analyses confirmed that IP-CHA is useful in the tissue engineering approach using MMCs, probably due to its well-organized interconnected porous structure.

The porous structure of IP-CHA was produced by a "foam-gel" technique using a cross-linking polyethyleneimine, enabling control of the pore size and porosity of IP-CHA. In the engineering of bone tissue, the ideal pore size is not clear, although some experiments suggest that a pore size of 200–400 μm is optimal for bone ingrowth (2,5,23). In this study, we used two different pore sizes of IP-CHA: HA150 with a mean pore diameter of 150 μm and HA300 with a mean diameter of 300 μm. Both HA150 and HA300 had the same porosity of 75%. As far as the mechanical properties are concerned, HA150 was superior to HA300 because the compressive strength of HA150 (10 MPa) is higher than that of HA300 (4 MPa) (unpublished data). Therefore, HA150 may be suitable material for bone reconstruction surgery, especially application in weight-bearing areas. An important question that remains, however, is whether the relatively small pore diameter of HA150 can support the osteogenic differentiation of MMCs. To address this point, we measured the level of ALP activity, the early marker of osteoblast differentiation, during in vitro culturing of MMCs in both HA150 and HA300. Both showed high levels of ALP activity with slightly higher levels of HA150 (Fig. 1). We also implanted these ceramics after culturing them with MMCs in Dex for 2 weeks (ceramics/MMCs/cult constructs) and measured

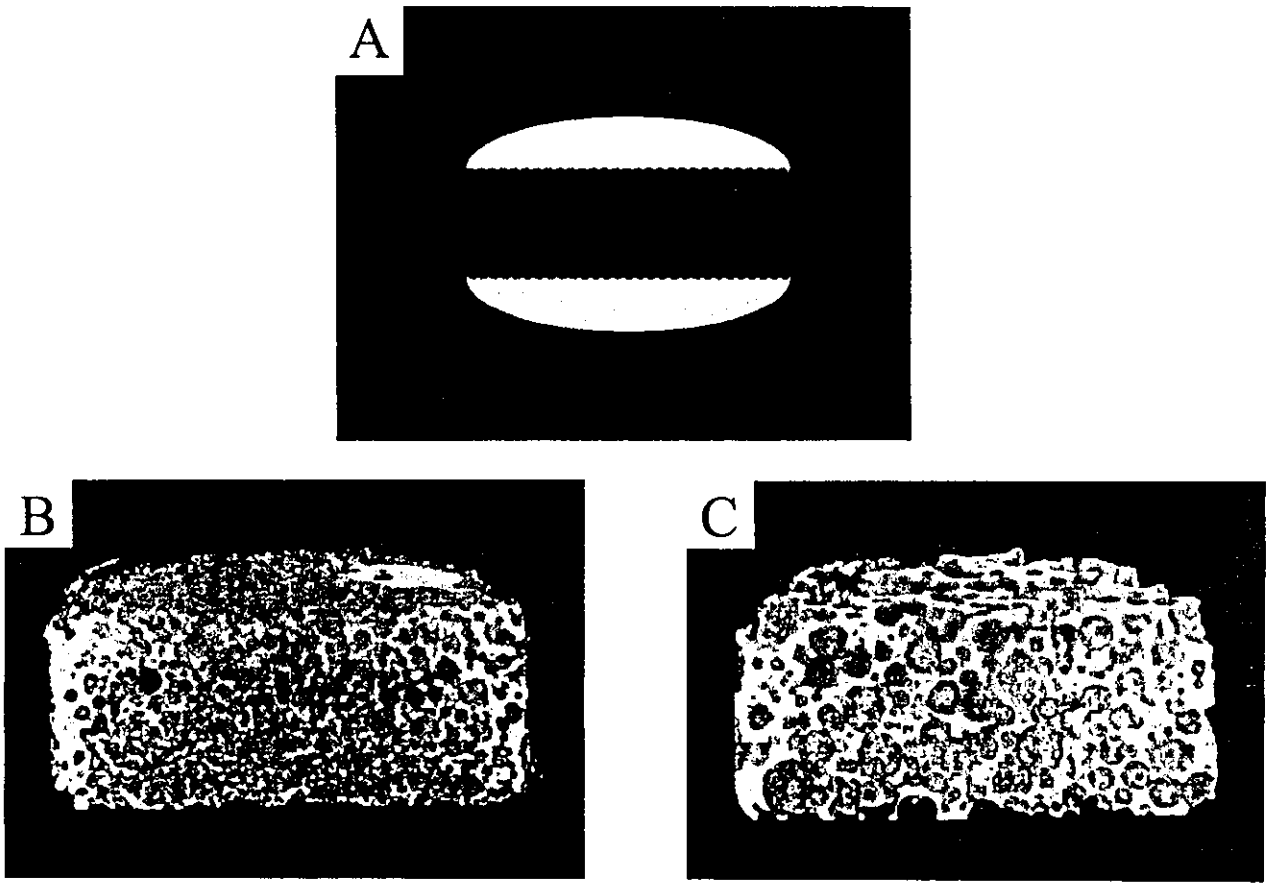

Figure 9. Three-dimensional distribution of newly formed bone in IP-CHA determined by Micro-CT analysis. (A) Illustration of the IP-CHA implant. The shaded area is the cross section of the implants. Three-dimensional micro-CT images at the cross section of the HA150/MMCs/cult (B) and HA300/MMCs/cult (C) 8 weeks after implantation. The three-dimensional (3D) image was constructed using the software, TRI3D-BON. The newly formed bone, originally represented in gray, now represented by orange.

the level of ALP activity and osteocalcin contents. Both the ALP activity and the osteocalcin contents of HA150/MMCs/cult were higher than those of HA300/MMCs/cult (Figs. 5 and 6). Micro-CT analysis also confirmed the comparable bone-forming capability of HA150/MMCs/cult to that of HA300/MMCs/cult (Fig. 9, Table 1). These results demonstrated that HA150 with a pore diameter of 150 μm can support the osteoblastic differentiation of MMCs and that the HA150/MMCs construct has more extensive bone-forming capability than does the HA300/MMCs/cult construct. Because of the high degree of mechanical properties of HA150, the HA150/MMCs/cult construct seems to be an ideal tool in bone reconstruction surgery.

Table 1. Bone Volumes of Various Constructs Determined by Micro-CT Analysis

	Bone Volume in Pore Areas (mm^3)
HA150/MMCs/cult ($n = 5$)	5.35 ± 2.36
HA300/MMCs/cult ($n = 5$)	4.26 ± 1.90
HA-A/MMCs/cult ($n = 5$)	1.88 ± 0.89*
HA-B/MMCs/cult ($n = 5$)	1.57 ± 0.60†
HA-C/MMCs/cult ($n = 5$)	0.52 ± 0.30†

Values are shown as mean ± SD. n: number of implants. There was no statistical difference between HA150/MMCs/cult and HA300/MMCs/cult.
*$p < 0.05$ vs. HA150/MMCs/cult and HA300/MMCs/cult.
†$p < 0.01$ vs. HA150/MMCs/cult and HA300/MMCs/cult.

CONCLUSIONS

IP-CHA is an excellent ceramic for use in bone tissue engineering because of its fully interconnected porous structure, which allows MMC dispersion and supports their osteogenic differentiation. Ceramics having pores with an average diameter of 150 μm, average interconnecting pore diameter of 40 μm, and 75% porosity (HA150) have a high level of mechanical strength. When cultured with MMCs for 2 weeks in vitamin C, glycerophosphate, and dexamethasone, HA150 has extensive in vivo capability for forming new bone. There-

fore, in combination with MMCs culture, HA150 could be an extremely useful tissue engineering material in bone reconstruction surgery.

ACKNOWLEDGMENTS: The authors thank Toshiba Ceramics Co., Ltd. for supplying materials and technical assistance, and K. Asai for histological technical assistance. This work was done by Three-Dimensional Tissue Module Project, METI (a Millennium Project).

REFERENCES

1. Ayers, R. A.; Simske, S. J.; Nunes, C. R.; Wolford, L. M. Long-term bone ingrowth and residual microhardness of porous block hydroxyapatite implants in humans. J. Oral Maxillofac. Surg. 56:1297–1301; 1998.
2. Boyan, B. D.; Hummert, T. W.; Dean, D. D.; Schwartz, Z. Role of material surfaces in regulating bone and cartilage cell response. Biomaterials 17:137–146; 1996.
3. Bucholz, R.; Carlton, A.; Holmes, R. Interporous hydroxyapatite as a bone graft substitute in tibial plateau fractures. Clin. Orthop. 240:53–62; 1988.
4. de Groot, K. Bioceramic consisting of calcium phosphate salts. Biomaterials 1:47–50; 1980.
5. Dennis, J. E.; Haynesworth, S. E.; Young, R. G.; Caplan, A. I. Osteogenesis in marrow-derived mesenchymal cell porous ceramic composites transplanted subcutaneously: Effect of fibronectin and laminin on cell retention and rate of osteogenic expression. Cell Transplant. 1:23–32; 1992.
6. Dohi, Y.; Ohgushi, H.; Tabata, S.; Yoshikawa, T.; Dohi, K.; Moriyama, T. Osteogenesis associated with bone Gla protein gene expression in diffusion chambers by bone marrow cells with demineralized bone matrix. J. Bone Miner. Res. 7:1173–1180; 1992.
7. Jarcho, M. Calcium phosphate ceramics as hard tissue prosthetics. Clin. Orthop. 157:259–278; 1981.
8. Kato, K.; Aoki, H.; Tabata, T.; Ogiso, M. Biocompatibility of apatite ceramics in mandibles. Biomater. Med. Devices Artif. Organs 7:291–297; 1979.
9. Maniatopoulos, C.; Sodek, J.; Melcher, A. H. Bone formation in vitro by stromal cells obtained from marrow of young adult rats. Cell Tissue Res. 254:317–330; 1988.
10. Nakano, K.; Harata, S.; Suetsuna, F.; Araki, T.; Itoh, J. Spinous process-splitting laminoplasty using hydroxyapatite spinous process spacer. Spine 17:S41–S43; 1992.
11. Ohgushi, H.; Goldberg, V. M.; Caplan, A. I. Heterotopic osteogenesis in porous ceramics induced by marrow cells. J. Orthop. Res. 7:568–578; 1989.
12. Ohgushi, H.; Goldberg, V. M.; Caplan, A. I. Repair of bone defects with marrow and porous ceramic. Acta Orthop. Scand. 60:334–339; 1989.
13. Ohgushi, H.; Okumura, M. Osteogenic capacity of rat and human marrow cells in porous ceramics. Acta Orthop. Scand. 61:431–434; 1990.
14. Ohgushi, H.; Dohi, Y.; Tamai, S.; Tabata, S. Osteogenic differentiation of marrow stromal stem cells in porous hydroxyapatite ceramics. J. Biomed. Mater. Res. 27:1401–1407; 1993.
15. Ohgushi, H.; Dohi, Y.; Katuda, T.; Tamai, S.; Tabata, S.; Suwa, Y. In vitro bone formation by rat marrow cell culture. J. Biomed. Mater. Res. 32:333–340; 1996.
16. Ohgushi, H.; Dohi, Y.; Yoshikawa, T.; Tamai, S.; Tabata, S.; Okunaga, K.; Shibuya, T. Osteogenic differentiation of cultured marrow stromal stem cells on the surface of bioactive glass ceramics. J. Biomed. Mater. Res. 32:341–348; 1996.
17. Ohgushi, H.; Yoshikawa, T.; Nakajima, H.; Tamai, S.; Dohi, Y.; Okunaga, K. Al2O3 doped apatite-wollastonite containing glass ceramic provokes osteogenic differentiation of marrow stromal stem cells. J. Biomed. Mater. Res. 44:381–388; 1999.
18. Ohgushi, H.; Caplan, A. I. Stem cell technology and bioceramics: From cell to gene engineering. J. Biomed. Mater. Res. 48:–913–927; 1999.
19. Reddi, A. H.; Sullivan, N. S. Matrix-induced endochondral bone differentiation: Influence of hypophysectomy, growth hormone, and thyroid-stimulating hormone. Endocrinology 107:1291–1299; 1980.
20. Tamai, N.; Myoui, A.; Tomita, T.; Nakase, T.; Tanaka, J.; Ochi, T.; Yoshikawa, H. Novel hydroxyapatite ceramics with an interconnective porous structure exhibit superior osteoconduction in vivo. J. Biomed. Mater. Res. 59:110–117; 2002.
21. Uchida, A.; Araki, N.; Shinto, Y.; Yoshikawa, H.; Kurisaki, H.; Ono, K. The use of calcium hydroxyapatite ceramic in bone tumor surgery. J. Bone Joint Surg. Br. 72: 298–302; 1990.
22. van Blitterswijk, C. A.; Hesseling, S. C.; Grote, J. J.; Koerten, H. K.; deGroot, K. The biocompatibility of hydroxyapatite ceramics: A study of retrieved human middle ear implants. J. Biomed. Mater. Res. 24:433–453; 1990.
23. Whang, K.; Thomas, C. H.; Healy, K. E.; Nuber, G. A novel method to fabricate bioabsorbable scaffolds. Polymer 36:837–842; 1995.
24. Yoshikawa, T.; Ohgushi, H.; Okumura, M.; Tamai, S.; Dohi, Y.; Moriyama, T. Biochemical and histological sequences of membranous ossification in ectopic site. Calcif. Tissue Int. 50:184–188; 1992.
25. Yoshikawa, T.; Ohgushi, H.; Tamai, S. Immediate bone forming capability of prefabricated osteogenic hydroxyapatite. J. Biomed. Mater. Res. 32:481–492; 1996.

Available online at www.sciencedirect.com
SCIENCE DIRECT®
Biochemical and Biophysical Research Communications 316 (2004) 943–948
BBRC
www.elsevier.com/locate/ybbrc

Three-dimensional visualization analysis of in vitro cultured bone fabricated by rat marrow mesenchymal stem cells☆

Takanori Kihara, Akira Oshima, Motohiro Hirose, and Hajime Ohgushi*

Tissue Engineering Research Center (TERC), National Institute of Advanced Industrial Science and Technology (AIST), 3-11-46 Nakoji, Amagasaki, Hyogo 661-0974, Japan

Received 13 February 2004

Abstract

Marrow mesenchymal stem cells are well known for their differentiation into bone-forming osteoblasts and in vitro mineralized tissue formation. However, process details, including tissue structure and cellular environments, remain unclear. The present study demonstrates three-dimensional visualization of tissue fabricated by culturing MSCs in the presence of calcein, a fluorescent marker for bone mineralization. The 3D visualization was performed by computer-assisted confocal laser scanning microscopy and revealed that the in vitro tissue consisted of layers of a mineralized matrix with round cells in the matrix lacunae, an unmineralized matrix (osteoid), and osteoblastic cells on the osteoid surface. The findings show that the mineralization by cultured MSCs is an in vitro counterpart of in vivo bone formation and indicate that the novel technique of visualization without tissue fixation could be useful for continuous monitoring of tissue organization in an ongoing culture.

Keywords: Mesenchymal stem cells; Osteogenic differentiation; Bone mineralization; Mineralized nodule; Calcein; Confocal laser scanning microscope; Three-dimensional visualization

Marrow mesenchymal stem cells (MSCs) are multipotent cells that differentiate into adipocytes, chondrocytes, and osteoblasts [1–5]. When MSCs are combined with a ceramic block and diffusion chamber, the composites are implanted into heterotopic sites, and can exhibit osteogenic potential resulting in bone formation in vivo [6–8]. MSCs can also differentiate into osteoblasts and undergo mineralization when they are cultured in the presence of ascorbic acid, β-glycerophosphate, and dexamethasone [9–11]. From studies of physicochemical and biochemical analyses, such mineralization is not a simple precipitation of calcium and phosphorus but is biological apatite, which is present in natural bone. Apatite formation is also associated with the formation of bone matrix protein [12]. Based on these analyses, in vitro mineralization derived from cultured MSCs can be characterized as "regenerative cultured bone."

New approaches for skeletal reconstruction have been proposed using cultured bone derived from patients' bone marrow cells [8,13,14]. Essential to the approach to advance this approach to wide-ranging clinical applications is confirmation that regenerative cultured bone is comparable to the composition of natural bone. The in vitro mineralized matrix produced by MSCs has been observed by methods involving histochemical staining and electron microscopic analyses [11,15,16]. However, it is difficult to continually observe the mineralization process during the culture periods because these methods require fixation and dehydration, which kill the cells. In other words, these processes neither allow further cultivation nor maintain its native composition. In addition, the three-dimensional (3D) analysis described later is not feasible using these conventional methods.

To confirm the structural similarity of the cultured bone to that of normal bone, an analysis of the spatial and functional relationships between the cultured cells

☆ Supplementary data associated with this article can be found, in the online version, at doi: 10.1016/j.bbrc.2004.02.134.

* Corresponding author. Fax: +81-6-6494-7861.
E-mail address: hajime-ohgushi@aist.go.jp (H. Ohgushi).

0006-291X/$ - see front matter © 2004 Elsevier Inc. All rights reserved.
doi:10.1016/j.bbrc.2004.02.134

and the extracellular matrix is required and, possibly, high resolution non-invasive technology is preferred. Confocal laser scanning microscopy (CLSM) is a very effective method for accomplishing this purpose. CLSM acquires a series of two-dimensional (2D) optical sections of the object and then creates a 3D reconstruction by stacking the 2D sections in sequence. Some have used this technique to observe a variety of cultured tissues [17,18], however no one has yet used CLSM to study mineralized tissue formed in vitro. The reason for this is the difficulty in developing the technology to emit fluorescence from the entire mineralized matrix area. To this end, we recently developed the new method of showing emissions of which intensity indicates the volume of the matrix [19]. This technology utilized in vitro mineralization by osteoblastic cell culture together with continuous administration of calcein, which binds to the entire mineralized matrix. Calcein is a fluorescent dye, which binds with high affinity to calcium and has been used to stain new bone growth in vivo [20–22]. Using this new method, we are able to observe calcein deposition in the mineralized matrix in vitro. In addition, we were able to confirm a quantitative correlation between calcein deposition and calcium contents [19]. Significantly, calcein administration to the cell culture did not affect cell viability and a comparable mineralized matrix formed without calcein administration. In this study, we analyzed the 3D structure of the cultured bone tissue using CLSM and investigated whether the in vitro structure is comparable to that of in vivo natural bone.

Materials and methods

Materials. Cell culture media and dexamethasone were purchased from Nacalai Tesque (Kyoto, Japan) and fetal bovine serum (FBS) was from JRH Biosciences (Lenexa, KS). Antibiotics were purchased from Sigma–Aldrich (St. Louis, MO). Phosphate-buffered saline (PBS), Trypsin–EDTA solution (0.05% trypsin, 0.53 mM EDTA-4Na), Hoechst 33258, Texas Red-phalloidin, and TOPRO-3 were purchased from Invitrogen (Carlsbad, CA). β-Glycerophosphate was purchased from Calbiochem (San Diego, CA). L-Ascorbic acid 2-phosphate magnesium salt *n*-hydrate (ascorbic acid-2-phosphate) was purchased from Wako Pure Chemical Industies (Osaka, Japan). Calcein was purchased from Dojindo Laboratories (Kumamoto, Japan). Fisher 344 male rats were purchased from Japan SLC (Shizuoka, Japan). *p*-Nitrophenylphosphate (PNPP) substrate was purchased from Zymed Laboratories (San Francisco, CA). Tissue culture flasks and plates were purchased from BD Biosciences (San Jose, CA) or Asahi Techno Glass (Chiba, Japan). Other reagents were purchased from Sigma–Aldrich or Nacalai Tesque.

Preparation and culture of rat MSCs. Rat MSCs were isolated and primary cultured as described previously [19]. In brief, bone marrow cells were obtained from the bone shaft of femora of 7-week-old rats. The cells were obtained from at least two rats and mixed. Then, mixed cells were seeded to 75 cm^2 tissue culture flask per femur. Primary cultures were maintained in a humidified atmosphere of 95% air and 5% CO_2 at 37 °C. Culture media were MEM (with Earle's salts and L-Gln) containing 15% FBS and antibiotics (100 U/mL penicillin G, 100 μg/mL streptomycin sulfate, and 0.25 μg/mL amphotericin B). In primary cultures, media were renewed three times per week. After confluence, cells were released from the substratum using Trypsin–EDTA solution and then seeded to 24-well tissue culture plates or 12-well tissue culture plates at 1.0×10^4 cells/cm^2. Under undifferentiated condition, the media were renewed three times per week using media supplemented with 82 μg/mL ascorbic acid-2-phosphate, 10 mM β-glycerophosphate, and 1 μg/mL calcein. Under osteogenic differentiation conditions, the above media were supplemented with 10 nM dexamethasone.

Measurements of ALP activities and DNA contents. The cell layers were washed twice with PBS and scraped off into 10 mM Tris-buffer (pH 7.4, 1 mM EDTA and 100 mM NaCl). The cell suspension was sonicated, after which 20 μL of sonicated suspension was used for DNA quantification. The quantification of the DNA contents was performed by using Hoechst 33258, with salmon sperm DNA used as standard. An aliquot (20 μL) of the suspension was mixed with 0.25 μg/mL Hoechst 33258 and incubated for 5 min at room temperature. The DNA measurements were done by fluorescence emission at 492 nm. Alkaline phosphatase (ALP) activity was determined as described by Reddi and Sullivan [23], with minor modifications. To measure the ALP activity, the same sonicated cell suspension was centrifuged at 13,000*g* for 1 min at 4 °C. An aliquot (20 μL) of the supernatant was mixed with PNPP substrate and incubated for 30 min at 37 °C. The ALP activity represented by amount of released *p*-nitrophenol was normalized to DNA contents. Triplicate determinations were used for each condition.

ALP activity and Alizarin red S staining. For ALP stain, cells were washed twice with PBS and fixed with 4% paraformaldehyde in 100 mM phosphate buffer (pH 7.3), then rinsed with AMP buffer (0.056 M 2-amino-2-methylpropansiol, pH 9.9) and stained with 0.5 mg naphthol-AS-MX phosphate sodium salt and 0.5 mg of fast red violet B/mL in AMP buffer for 5 min. After staining cells were rinsed with PBS. For Alizarin red S stain, cells were washed twice with PBS and fixed with 95% ethanol, then rinsed with water and stained with Alizarin red S (5 mg/mL in PBS) for 4 min. After staining cells were rinsed with water. Samples were observed by phase contrast microscope Olympus CK40 (Olympus, Tokyo, Japan).

Quantitative fluorescence analysis of calcein. The fluorescence of the calcein incorporated into the mineralized matrices was visualized/quantified by using a fluorescence image analyzer Typhoon 8600 (Molecular Dynamics, CA, USA) and was also observed by fluorescence microscope Olympus IX70 (Olympus, Tokyo, Japan) equipped with a B/W CCD digital camera ORCA-ER (Hamamatsu Photonics, Shizuoka, Japan), or confocal laser scanning microscope (CLSM) LSM510 system (Carl Zeiss, Germany).

Fluorescence staining. Cells were washed with PBS, fixed with 95% ethanol at 4 °C for 15 min, and permeabilized with 0.5% Triton X-100 at room temperature for 5 min. Cells were stained with Texas Red-phalloidin for actin microfilaments and with nuclear dye TOPRO-3 at room temperature for 60 min. The specimens were viewed with CLSM.

CLSM analysis and three-dimensional reconstruction images. Fluorescence of serial sections was observed by using CLSM (Table 1). The thickness of the X–Y section was 0.9 μm and the interval of the continuous sections was 0.45 μm. Three-dimensional images were reconstructed by layering a series of X–Y sections using "TRI/3D-BON" computer graphics software (Ratoc System Engineering, Japan).

Table 1
Specification of CLSM system

	Excitation laser		Emission pass filter
	Laser unit	Wave length (nm)	
Calcein	Argon	488	BP 505–530
Texas red	HeNe	543	BP 560–615
TOPRO-3	HeNe	633	LP 650

The nodules were observed at 21 areas in four individual experiments. We showed one of the nodules structure in this study.

Results and discussion

After 7 days of culture, rat MSCs cultured under osteogenic differentiation conditions showed high ALP activity, one of the markers for osteoblast differentiation (Fig. 1A). Clusters of many cuboid-shaped cells were seen after 7 days of culture. The center of the cluster appeared to be an amorphous mineralized area (nodule). After 14 days of culture, the number of clusters had increased and numerous nodules could be seen (Fig. 1B). These nodules were stained with Alizarin red S, which is widely used as an indicator of mineralization (Fig. 1C). High ALP activity in these areas including the surrounding cellular regions was also detected (Fig. 1D). Moreover, these nodules incorporated calcein, and the level of incorporation increased in a time-dependent manner (Figs. 1E and F). These results indicate that rat MSCs differentiated into osteoblasts and formed mineralized nodules. The process of nodule formation was similar to that without the addition of calcein into the culture medium (data not shown). Therefore, the amount of calcein used in this experiment did not

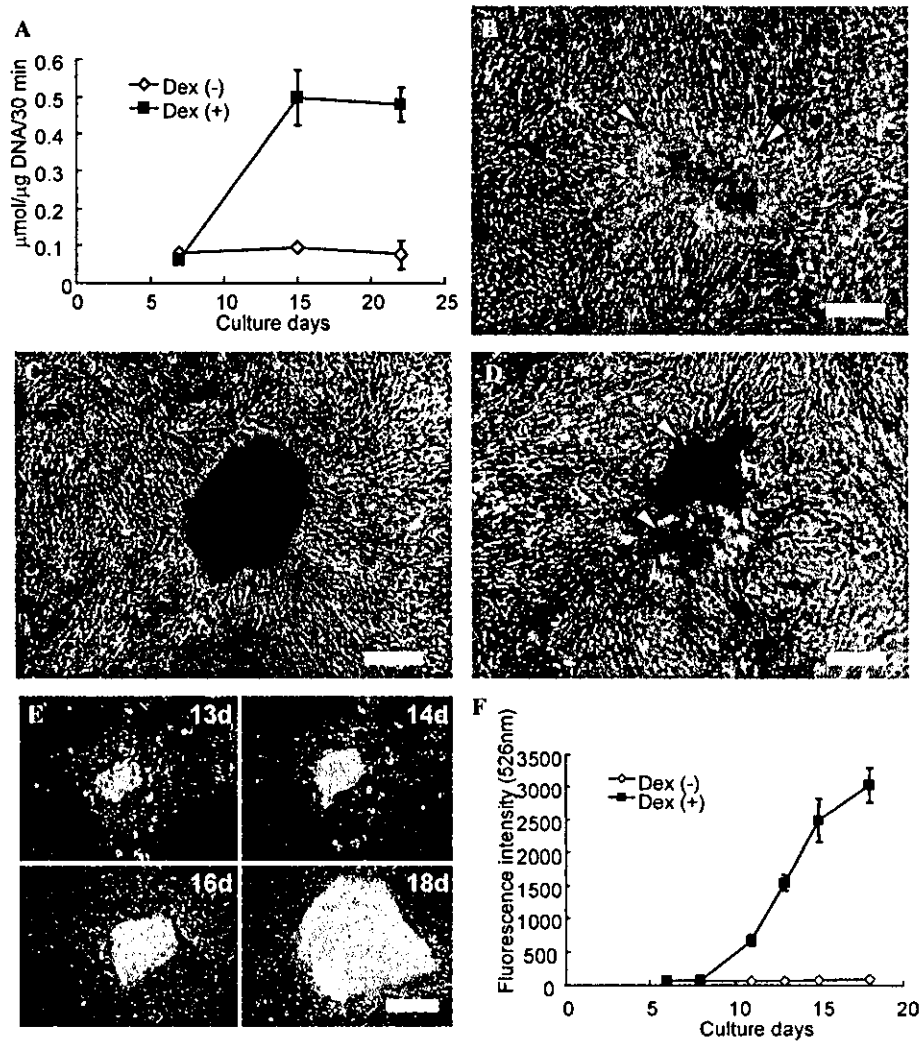

Fig. 1. Differentiation of MSCs into osteoblasts. Cells were cultured under osteogenic differentiation conditions, Dex (+), or undifferentiated condition, Dex (−). The values are means ± SD of experiments run in triplicate. (A) ALP activities during the culture periods. After 7 days of culture, MSCs cultured under differentiation conditions showed higher ALP activity than did those in the undifferentiated condition. (B) Phase contrast microscopy of differentiated MSCs. Mineralized nodules are seen in the center of the clustered cells (arrowheads). (C) Phase contrast microscopy of the cultured cell layer stained with Alizarin red S. The stained area suggests the presence of calcium. (D) Phase contrast microscopy of the cell layer with marked ALP activity. The clustered cells and mineralized area show high ALP activity, represented in red (arrowheads). (E) Merged image of fluorescence microscopy of accumulated calcein (green) and phase contrast microscopy (gray scale) of the same region of the cell layer. Images were taken at the same nodule at 13, 14, 16, and 18 days. The calcein-positive regions are shown on the cell cluster and increased in a time-dependent manner. (F) Quantification of accumulated calcein in the mineralized matrices. Calcein depositions under osteogenic differentiation conditions increased in a time-dependent manner. All images were taken at 14 days under differentiation conditions. Bar, 200 μm.

impede the osteoblastic differentiation of MSCs. The use of CLSM enabled direct observation of calcein uptake in the nodules without fixing the culture specimen. Therefore, we were able to monitor the natural mineralization process at any time of the culture period and to reconstruct the 3D pattern of mineralization, as described later. The calcein deposition increased after 7 days of culture, and the nodule grew large enough to be analyzed at 14 days of culture. Consequently, we used the specimens after 14 days of culture in the following studies.

There are limitations in light and electron microscopic analyses in obtaining 3D structural information in the process of mineralization such as extracellular mineralized matrix patterns and cell location in the microenvironments. We tried to overcome these disadvantages and finally succeeded in visualizing the structure using CLSM (Fig. 2). The cells were visualized by actin and nuclear staining. From the 2D image of the X–Z section, we found that the mineralized matrix lay on and contacted the bottom of the culture plate; the surface area of the nodule was covered with numerous cells (100% of 21 nodules). The surface cell layer was about 9 μm thick and a thin interval, 2.7 μm thick, with little uptake of calcein was seen between the cell layer and the mineralized matrix. This thin interval would be unmineralized bone matrix (i.e., osteoid) [15]. The osteoid thickness of the proximal tibia of normal rats is 1.82 ± 1.90 μm [24]. Thus, the osteoid constructed by the cultured MSCs was comparable to natural bone osteoid. Some round-shaped cells were present inside the mineralized matrix (71% of 21 nodules) (Fig. 2B). These cells were clearly distinct from the cells of the surface cell layer on the mineralized matrix. The cells on the matrix had stretched actin filaments, but the cells within the mineralized matrix did not (Figs. 2B and C).

To analyze the structure of the nodules in detail, we created a 3D graphic from a stack of 2D slices collected by CLSM giving a bird's eye view using computer graphics techniques. Fig. 3A shows the top surface of the nodule, which was completely covered with clusters of cells. From this 3D graphic, not only could we extract any specific 2D sections, we can also observe the entire nodule from any angle (Figs. 3B and C). As shown in Fig. 3C (view looking up), the bottom of the mineralized matrix was in direct contact with the culture plate. In the mineralized areas seen as green, few of the round-shaped cells could be detected. They were entirely embedded in the lacunae of the matrix and each cell was completely isolated from the others (see Movie 1 online). When the image of the cells in the 3D reconstructed graphic was separated from the mineralized matrix, the dendritic morphology with short processes could be seen (Fig. 3D). Hence, their morphology was clearly different from that of the spreading cells on the top surface of the nodules. The cross-sectional area of each of the round-shaped cells in the matrix was $57 \pm 6.8\ \mu m^2$ ($n = 3$) and the volume was $485 \pm 102\ \mu m^3$ ($n = 3$). From confocal laser scanning microscopic analysis of natural bone, it is reported that osteocytes could be observed in the mineralized matrix and that they have many processes with dendritic morphology [25]. The cross-sectional area of osteocyte lacunae in normal trabecular bone ranges between 50.6 and $53.8\ \mu m^2$ [26]. Together with these reports, our findings indicate that the round-shaped cells

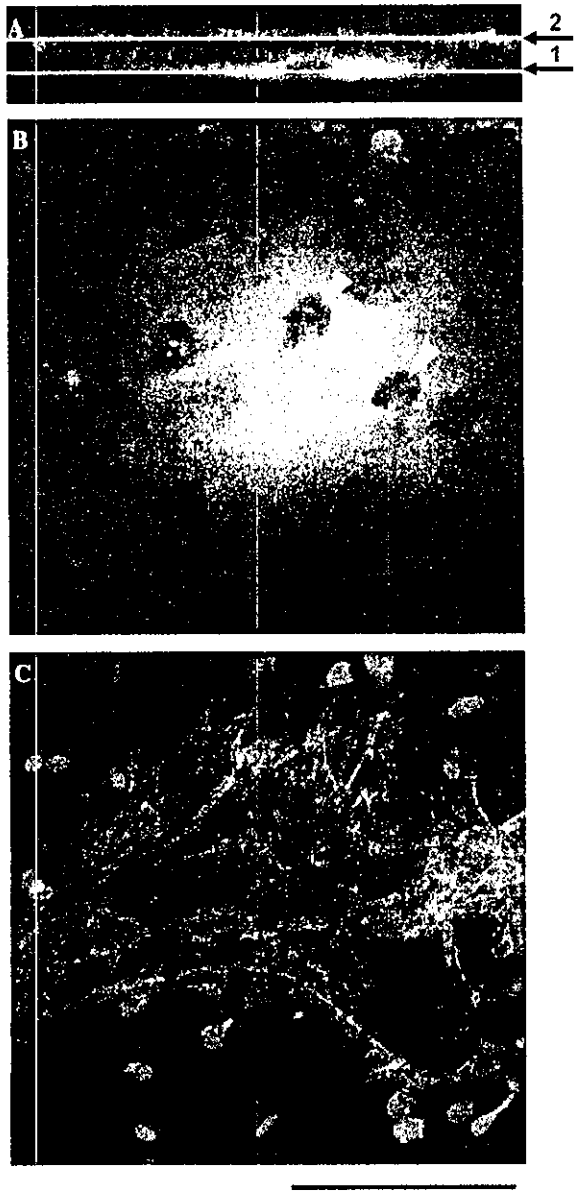

Fig. 2. Confocal laser scanning microscopy of the mineralized nodule area. (A) Image of confocal X–Z section obtained along the plane across one of the mineralized nodules. Confocal X–Y sectional views of mineralized matrix region (B, $h = 4.95$ μm from the base) and outer surface region (C, $h = 19.8$ μm from the base) of the nodule. (B) was taken as line 1 in (A), and (C) was taken as line 2. The mineralized matrix is indicated by green, the actin microfilaments by red, and the nuclei by blue. The round-shaped cells lay in the mineralized matrix (arrowheads). Bar, 100 μm.

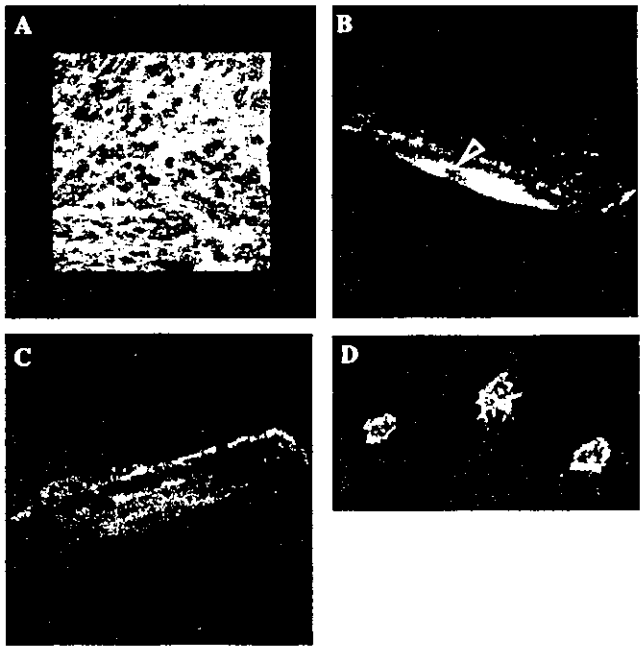

Fig. 3. Three-dimensional computer graphic of mineralized nodule area. (A) Top surface of the nodule. (B) Bird's eye view of the nodule taken from the upper right portion of (A). The graphic was observed from an oblique angle. A round-shaped cell is embedded in the lacunae of the mineralized matrix (arrowhead). (C) Graphic obtained from a different projection angle in (B). (D) The round-shaped cells in the mineralized matrix were extracted from the 3D computer graphic of the nodule.

with short processes in the matrix lacunae are osteocytes that differentiated from osteoblasts originally localized on the nodule surface.

Taken together, we propose the following overall process of mineralized nodule formation. Initially, a number of MSCs expand and cover the culture plate surface. They differentiate into osteoblasts and organize into an unmineralized matrix. Matrix mineralization (mineralization front) occurs at the surface of the culture plate and thus the osteoblasts are lifted after this mineralization. Some osteoblasts remain in the mineralized matrix and further differentiate into osteocytes. This mineralization process of in vitro bone tissue is similar to that of in vivo natural bone regeneration such as appositional bone formation. Therefore, the in vitro mineralization is a counterpart of the in vivo bone formation and can be considered as regenerative cultured bone.

The present results clearly show that the in vitro process of forming mineralized tissue (cultured bone) by MSCs is similar to the natural occurrence as seen in in vivo bone tissue regeneration and confirm that the structure of the in vitro tissue is comparable to normal in vivo bone tissue. The confirmation was accomplished by our novel approach using CLSM, which depicts direct visualization of the 3D structure of the mineralized tissue. Furthermore, this system of 3D visualization using calcein and CLSM enables continuous observation of the same sample during the culture period. This real-time monitoring system could be a useful tool for confirming the mechanism used by cells to organize into in vitro tissue.

Acknowledgments

This work was supported by the Three-Dimensional Tissue Module Project, METI (A Millennium Project) and by a Grant-in-Aid for Scientific Research from the Ministry of Education, Science, Sports and Culture (MEXT).

References

[1] M. Owen, A.J. Friedenstein, Stromal stem cells: marrow-derived osteogenic precursors, Ciba Found. Symp. 136 (1988) 42–60.
[2] M.C. Galmiche, V.E. Koteliansky, J. Briere, P. Herve, P. Charbord, Stromal cells from human long-term marrow cultures are mesenchymal cells that differentiate following a vascular smooth muscle differentiation pathway, Blood 82 (1993) 66–76.
[3] S.P. Bruder, D.J. Fink, A.I. Caplan, Mesenchymal stem cells in bone development, bone repair, and skeletal regeneration therapy, J. Cell Biochem. 56 (1994) 283–294.
[4] M.F. Pittenger, A.M. Mackay, S.C. Beck, R.K. Jaiswal, R. Douglas, J.D. Mosca, M.A. Moorman, D.W. Simonetti, S. Craig, D.R. Marshak, Multilineage potential of adult human mesenchymal stem cells, Science 284 (1999) 143–147.
[5] Y. Jiang, B.N. Jahagirdar, R.L. Reinhardt, R.E. Schwartz, C.D. Keene, X.R. Ortiz-Gonzalez, M. Reyes, T. Lenvik, T. Lund, M. Blackstad, J. Du, S. Aldrich, A. Lisberg, W.C. Low, D.A. Largaespada, C.M. Verfaillie, Pluripotency of mesenchymal stem cells derived from adult marrow, Nature 418 (2002) 41–49.
[6] H. Ohgushi, V.M. Goldberg, A.I. Caplan, Heterotopic osteogenesis in porous ceramics induced by marrow cells, J. Orthop. Res. 7 (1989) 568–578.
[7] Y. Dohi, H. Ohgushi, S. Tabata, T. Yoshikawa, K. Dohi, T. Moriyama, Osteogenesis associated with bone gla protein gene expression in diffusion chambers by bone marrow cells with demineralized bone matrix, J. Bone Miner. Res. 7 (1992) 1173–1180.
[8] H. Ohgushi, A.I. Caplan, Stem cell technology and bioceramics: from cell to gene engineering, J. Biomed. Mater. Res. 48 (1999) 913–927.
[9] C. Maniatopoulos, J. Sodek, A.H. Melcher, Bone formation in vitro by stromal cells obtained from marrow of young adult rats, Cell Tissue Res. 254 (1988) 317–330.
[10] P.S. Leboy, J.N. Beresford, C. Devlin, M.E. Owen, Dexamethasone induction of osteoblast mRNAs in rat marrow stromal cell cultures, J. Cell Physiol. 146 (1991) 370–378.
[11] J.E. Davies, R. Chernecky, B. Lowenberg, A. Shiga, Deposition and resorption of calcified matrix in vitro by rat marrow cells, Cells Mater. 1 (1991) 3–15.
[12] H. Ohgushi, Y. Dohi, T. Katuda, S. Tamai, S. Tabata, Y. Suwa, In vitro bone formation by rat marrow cell culture, J. Biomed. Mater. Res. 32 (1996) 333–340.
[13] R.F. Service, Tissue engineers build new bone, Science 289 (2000) 1498–1500.
[14] J. Ringe, C. Kaps, G.R. Burmester, M. Sittinger, Stem cells for regenerative medicine: advances in the engineering of tissues and organs, Naturwissenschaften 89 (2002) 338–351.
[15] J.E. Davies, P. Ottensmeyer, X. Shen, M. Hashimoto, S.A.F. Peel, Early extracellular matrix synthesis by bone cells, in: J.E. Davies

(Ed.), In the Bone–Biomaterial Interface, University of Toronto Press, Toronto, 1991, pp. 214–228.
[16] B. Lowenberg, A. Chernecky, A. Shiga, J.E. Davies, Mineralized matrix production by osteoblasts on solid titanium in vitro by rat marrow cells, Cells Mater. 1 (1991) 177–187.
[17] O. Simonetti, A.J. Hoogstraate, W. Bialik, J.A. Kempenaar, A.H. Schrijvers, H.E. Bodde, M. Ponec, Visualization of diffusion pathways across the stratum corneum of native and in-vitro-reconstructed epidermis by confocal laser scanning microscopy, Arch. Dermatol. Res. 287 (1995) 465–473.
[18] A.V. Andjelkovic, M.R. Zochowski, F. Morgan, J.S. Pachter, Qualitative and quantitative analysis of monocyte transendothelial migration by confocal microscopy and three-dimensional image reconstruction, In Vitro Cell Dev. Biol. Anim. 37 (2001) 111–120.
[19] E. Uchimura, H. Machida, N. Kotobuki, T. Kihara, S. Kitamura, M. Ikeuchi, M. Hirose, J. Miyake, H. Ohgushi, In-situ visualization and quantification of mineralization of cultured osteogenetic cells, Calcif. Tissue Int. 73 (2003) 575–583.
[20] V.C. Chiu, D.H. Haynes, High and low affinity Ca^{2+} binding to the sarcoplasmic reticulum: use of a high-affinity fluorescent calcium indicator, Biophys. J. 18 (1977) 3–22.
[21] M. Okumura, H. Ohgushi, S. Tamai, Bonding osteogenesis in coralline hydroxyapatite combined with bone marrow cells, Biomaterials 12 (1991) 411–416.
[22] T. Yoshikawa, H. Ohgushi, S. Tamai, Immediate bone forming capability of prefabricated osteogenic hydroxyapatite, J. Biomed. Mater. Res. 32 (1996) 481–492.
[23] A.H. Reddi, N.E. Sullivan, Matrix-induced endochondral bone differentiation: influence of hypophysectomy, growth hormone, and thyroid-stimulating hormone, Endocrinology 107 (1980) 1291–1299.
[24] L.L. Lee, J.S. Lee, S.D. Waldman, R.F. Casper, M.D. Grynpas, Polycyclic aromatic hydrocarbons present in cigarette smoke cause bone loss in an ovariectomized rat model, Bone 30 (2002) 917–923.
[25] H. Kamioka, T. Honjo, T. Takano-Yamamoto, A three-dimensional distribution of osteocyte processes revealed by the combination of confocal laser scanning microscopy and differential interference contrast microscopy, Bone 28 (2001) 145–149.
[26] V. Cane, G. Marotti, G. Volpi, D. Zaffe, S. Palazzini, F. Remaggi, M.A. Muglia, Size and density of osteocyte lacunae in different regions of long bones, Calcif. Tissue Int. 34 (1982) 558–563.

Available online at www.sciencedirect.com
SCIENCE DIRECT®
Materials Science and Engineering C 24 (2004) 437–440
MATERIALS SCIENCE & ENGINEERING C
www.elsevier.com/locate/msec

Bone tissue engineering based on bead–cell sheets composed of calcium phosphate beads and bone marrow cells

Katsuko S. Furukawa[a,*], Shunsuke Miyauchi[a], Daisuke Suzuki[a], Yoshikazu Umezu[b], Tsuneo Shinjo[b], Takashi Ushida[a], Miki Eguchi[b], Tetsuya Tateishi[a,c]

[a] *Biomedical Engineering (Ushida and Furukawa), Laboratory, Department of Mechanical Engineering, Graduate School of Engineering, University of Tokyo, 503, 8th Building, 7-3-1 Hongo, Bunkyo, Tokyo 113-8656, Japan*
[b] *Advance Co., Saitama, Japan*
[c] *Biomaterials Center, National Institute for Materials Science, Ibaraki, Japan*

Received 29 August 2003; received in revised form 30 August 2003; accepted 23 November 2003

Abstract

We developed a new tissue-engineered bone graft model composed of bovine bone marrow stromal cells (BMSCs), and beta tricalcium phosphate (beta TCP) porous beads. Such cell–bead sheets were prepared by means of cultivation of BMSCs with the beads in alpha-MEM culture medium supplemented with 10% fetal bovine serum. The shape of the sheets was possible to change depending on that of a plastic mold having a circle or quadrangle shape. Addition of poundage on the overlaid cell–bead sheets induced the connection of these sheets with each other, and achievement of thicker implant formation. A nonwoven fabric sheet of poly-L-lactic acid (PLLA) could also be inserted in between each cell–bead sheet. Consequently, bone implants having a size of 20 × 20 × 5 mm were successfully developed. This kind of techniques would be useful in thick implants for other tissue implants.

Keywords: Bone tissue engineering; Sheet; Beads; Bone marrow cells

1. Introduction

There is an increasing demand for establishment of treatments in the repair of osseous defects caused by trauma or tumor resection. Allogeneic or xenogeneic bones could be considered as a substitute for a patient's bone, but their use is limited because of the immunologic rejection. In addition, a series of large bone defects caused severe difficulties in using autologous tissue [1]. Therefore, artificial bones composed of metals such as aluminum, stainless, or titanium have been applied for the patients, but the implants still have many problems. Such metal-based artificial bones with inappropriate mechanical properties that differ from that of natural bones induce abrasion, attrition, and/or absorption in the original bone of the patients around the implanted artificial bone [2]. These facts give rise to strong expectations for development of tissue-engineered artificial bones, similar in mechanical properties of natural bones.

In the field of bone tissue engineering, there is a limitation in the size of the implant. When we had an attempt to make a bone implant with larger sizes, it was difficult to realize homogenous inoculation of the cells, particularly in the center of the scaffold [3]. Although it could involve a lot of cells into the center of the scaffold, necrosis may develop most often in the center due to limitations in diffusion of the oxygen and nutrition. Therefore, the present study was designed to make a new bone implant that has a lager size than that of a previously reported one [4,5], and a large number of cells even in the center of the implant.

2. Materials and methods

2.1. Preparation of porous beads composed of calcium phosphates

Aqueous slurry of calcium phosphates and a binder reagent were mixed in a ultrasonic homogenizer and air

* Corresponding author. Tel.: +81-3-5841-6331; fax.: +81-3-5841-6442.
E-mail address: furukawa@mech.t.u-tokyo.ac.jp (K.S. Furukawa).

0928-4931/$ - see front matter © 2004 Elsevier B.V. All rights reserved.
doi:10.1016/j.msec.2003.11.010